Environmental Science & Technology

Article

pubs.acs.org/est

Measuring Particulate Emissions of Light Duty Passenger Vehicles Using Integrated Particle Size Distribution (IPSD)

David C. Quiros,*[,†,‡] Sherry Zhang,[†] Satya Sardar,[†] Michael A. Kamboures,[†] David Eiges,[†] Mang Zhang,[†] Heejung S. Jung,[§] Michael J. Mccarthy,[†] M.-C. Oliver Chang,[†] Alberto Ayala,[†] Yifang Zhu,[‡,∥] Tao Huai,[†,∥] and Shaohua Hu[†]

[†]California Air Resources Board 1001 I Street, Sacramento, California 95814, United States

[‡]Environmental Science & Engineering, Institute of the Environment and Sustainability, La Kretz Hall, Suite 300, Los Angeles, California 90095, United States

[§]Center for Environmental Research and Technology (CE-CERT), Bourns College of Engineering, University of California, Riverside, 1084 Columbia Avenue Riverside, California 92507, United States

[∥]Department of Environmental Health Sciences, Fielding School of Public Health, University of California, Los Angeles 650 Charles E. Young Drive South, Los Angeles, California 90095, United States

Supporting Information

ABSTRACT: The California Air Resources Board (ARB) adopted the low emission vehicle (LEV) III particulate matter (PM) standards in January 2012, which require, among other limits, vehicles to meet 1 mg/mi over the federal test procedure (FTP). One possible alternative measurement approach evaluated to support the implementation of the LEV III standards is integrated particle size distribution (IPSD), which reports real-time PM mass using size distribution and effective density. The IPSD method was evaluated using TSI's engine exhaust particle sizer (EEPS, 5.6−560 nm) and gravimetric filter data from more than 250 tests and 34 vehicles at ARB's Haagen-Smit Laboratory (HSL). IPSD mass was persistently lower than gravimetric mass by 56−75% over the FTP tests and by 81−84% over the supplemental FTP (US06) tests. Strong covariance between the methods suggests test-to-test variability originates from actual vehicle emission differences rather than measurement accuracy, where IPSD offered no statistical improvement over gravimetric measurement variability.

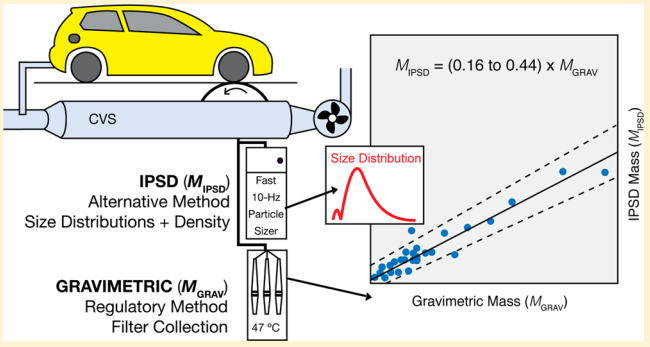

1. INTRODUCTION

Chronic exposure to ambient particulate matter (PM), a mixture of natural and anthropogenic solid and semivolatile constituents, is associated with increased cardiopulmonary morbidity and mortality.[1,2] Exposure to primary PM from mobile sources has been well characterized,[3−9] and has been linked directly to adverse health outcomes.[10−12] Over the past decades, the California Air Resources Board (ARB) has implemented several mobile source control programs resulting in widespread emission reductions,[13] and ARB adopted PM standards for the low emission vehicle (LEV) III standards as part of the Advanced Clean Cars program. Beginning with model year (MY) 2017 and MY 2025, the current 10 mg/mi PM standards will decrease to 3 mg/mi and 1 mg/mi, respectively, over the Federal Test Procedure (FTP).[14] LEV III standards also include PM standards applicable to the Supplemental FTP (US06) test cycle, as well as higher interim in-use emission limits.

One stated objective of the LEV III standards was to ensure future vehicles continue to have very low PM emissions. Current gasoline vehicles commonly use port-fuel injection (PFI) and typically overcomply with the current 10 mg/mi standard. However, some newer technologies being introduced to meet increasingly stringent greenhouse gas emission standards, such as gasoline direct injection (GDI), have been shown to comply by a smaller margin[15−17] and the measurement precision at the new standards, especially at 1 mg/mi, was not thoroughly investigated. Since the adoption of the LEV III standards, ARB has confirmed the feasibility of gravimetric measurement of PM emissions below 1 mg/mi using the existing filter-based gravimetric method.[18] PM emission standards in the United States have thus far been defined on a filter-based mass basis, which to date remains the reference method for measuring PM. Nevertheless, alternative metrics used to define, measure, and control PM emissions is critical to

Received: February 5, 2015
Revised: April 15, 2015
Accepted: April 16, 2015
Published: April 16, 2015

DOI: 10.1021/acs.est.5b00666
Environ. Sci. Technol. 2015, 49, 5618−5627

further understand the nature of PM emissions emitted by vehicles compliant to today's most stringent emission standards.

One promising alternative approach for measuring PM mass from light-duty vehicles is integrated particle size distribution (IPSD),[19−21] a method where real-time mobility-based particle size distributions[22−24] are converted into mass distributions by applying size-resolved particle effective density.[25−28] Previously, the IPSD method, reporting suspended PM mass, has shown reduced test-to-test variability relative to a filter-based gravimetric reference mass and has exhibited a one-to-one relationship relative to gravimetric mass when measuring heavy-duty diesel truck emissions.[19,20,29] Effective density of particulate emissions from light-duty gasoline vehicles has been measured by Maricq and Xu (2004);[25] and, more recently redefined by Quiros et al.[30] for modern GDI and PFI gasoline vehicles, and a light-duty diesel vehicle (LDD) with a diesel particulate filter (DPF). The primary objective of this study is to evaluate the IPSD method for estimating suspended PM mass (M_{IPSD}) compared to the filter-based gravimetric mass defined by the CFR Part 1065 specifications (M_{GRAV}). We test this hypothesis using a comprehensive of particle size distribution data measured using the TSI EEPS (engine exhaust particle sizer, 5.6−560 nm) from 168 FTP and 87 US06 tests, and 34 different vehicles that included PFI, GDI, and LDD technologies.

Although inconclusive, some studies suggests health effects are also associated with alternative metrics such as total or ultrafine particle (UFP, <100 nm) number concentration[31−33] and active or Fuchs surface area.[34−37] Accordingly, this work evaluates trends using estimates of total particle number (N_{IPSD}) and active surface area (SA_{IPSD}) using the same EEPS distributions. In addition to trends in total number and active surface area calculated over the entire measurement range of the EEPS (5.6−560 nm), active surface area and number are reported by size bin (e.g., SA_{IPSD} < 23 nm or N_{IPSD} < 100 nm).

2. MATERIALS AND METHODS

Testing was conducted at the ARB Haagen-Smit Laboratory (HSL) in El Monte, CA. Data were collected in three of the light-duty test cells equipped with a 48 in. single-roll electric chassis dynamometer, a constant volume sampler (CVS), and a PM sampling system that meets requirements defined by 40 CFR 1065.[38] Each test included gravimetric filter sampling using Polytetrafluoroethylene (PTFE) media downstream of a cyclone ($d_{50} \approx 2.5$ μm and >99% penetration of submicron particles). A more detailed description of the test cells and test procedures can be found in Hu et al.[18] An FTP test includes a cold-start urban dynamometer driving schedule (UDDS) and a hot-start UDDS weighted by 0.43 and 0.57, respectively. This study included both three-filter and two-filter tests as defined in CFR Part 1066.801(b) options 1 and 2, respectively.[39] Tunnel blank filters were collected at test-cell ambient temperature, but dilution-air subtraction was not conducted to better understand emissions variability without selecting, and presenting results from, a specific subtraction method. US06 tests were measured using a single filter following an initial US06 preconditioning cycle followed by 90 s of neutral idling without restarting the engine. Test fuels included California certification- and commercial-grade gasoline containing between 0 and 10% ethanol, and California commercial-grade diesel (<15 ppm sulfur). Complete test lists are located in Tables S1 and S2 in the Supporting Information.

Four TSI EEPS units were deployed in three test cells concurrently over a few years that ran firmware versions between 3.05 and 3.11. The EEPS uses a unipolar diffusion and field charger that generates a positive corona to induce a high degree of charge onto particles, which are then classified using 22 electrodes providing size distribution over 32 channels.[23] Gravimetric and suspended PM was measured using a cyclonic separator with >99% penetration of 1 μm particles ($d_{50} \approx 2.5$ μm); no additional dilution or sample flow heating was used. The manufacturer maintenance procedures were followed, including regular cleaning of the electrode surfaces, using an acrylic cylinder and a lint-free cloth, and charging needles using forceps. A small portion of PM mass and size distribution data were rejected for violation of PM sampling criteria (e.g., filter temperature violation) or EEPS errors (e.g., flow or charger voltage errors). The EEPS has been widely used to measure transient particle size distribution,[40,41] but it has been shown to underestimate the concentration of fractal-like exhaust particles with diameters greater than 100 nm compared to measurements from an SMPS.[22,24,29,42,43] To minimize some sizing bias associated with using the EEPS, but not introduce additional variability between vehicles, each size distribution was corrected using the identical average SMPS-to-EEPS log-normal ratio determined using a comprehensive evaluation of light-duty vehicles under various low- and high-load steady-state driving conditions representing all the range of conditions of the FTP and US06 test cycles.[30] All data in this paper reflect this correction, which resulted in approximately ten percent higher calculated PM mass (M_{IPSD}) than uncorrected distributions (Figure S1, in the Supporting Information).

Size distributions were used to estimate three IPSD parameters: total number (N_{IPSD}); active surface area (SA_{IPSD}) by weighting mobility diameter (d_p) by an exponent of 1.4;[36,44] and, particle mass (M_{IPSD}) following eq 1:

$$M_{IPSD} = \sum_i \left[\rho_{eff,i} \times \left(\frac{\pi}{6} {d_{p,i}}^3 \right) \times n_i \right] \quad (1)$$

where $\rho_{eff,i}$ is the particle effective density, d_p is the mobility diameter, and n_i is the measured number concentration for size bin i. IPSD calculations were derived from EEPS measurements of diluted vehicle exhaust, whereas gravimetric measurements and CVS parameters are reported at standard conditions (T = 293.15 K and P = 1013 mbar). Therefore, the EEPS measurements were corrected to standard conditions following the ideal gas law using the proportionality of pressure (P), volume, and temperature (T), which experimentally resulted in 3.0 ± 0.6% and 7.1 ± 2.0% average calculated mass increases for the FTP and US06 tests, respectively.

Effective density was calculated and applied using the power fit law presented in eq 2 and functions shown in Supporting Information Figure S2.

$$\rho_{eff} = 1000 \times c \times d_p^{D_m - 3} \quad (2)$$

Effective density (kg/m^3) is a function of electrical mobility diameter d_p (nm), a constant c (dimensionless), and mass-mobility scaling exponent (D_m). An exponential model fits well to measured effective densities for the nucleation mode;[20,21] however, as particle size increases, experimental measurements deviated from fits. Because mass yielded by the IPSD method is heavily dependent upon the accuracy of effective densities reported near the mass median diameter (MMD), a power fit law, expressed by eq 2, was used to model the effective densities

DOI: 10.1021/acs.est.5b00666
Environ. Sci. Technol. 2015, 49, 5618−5627

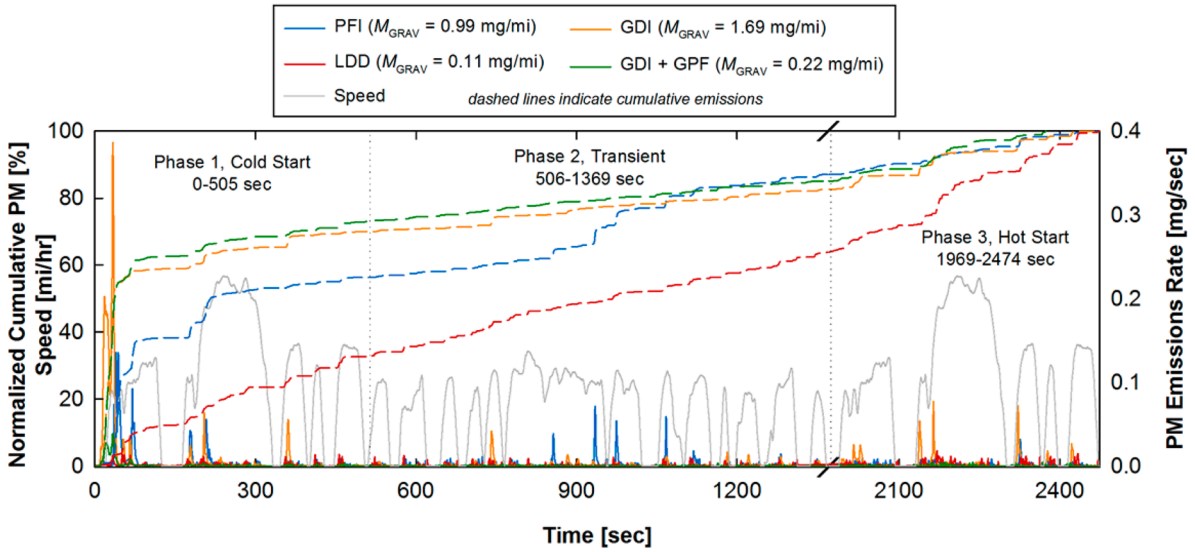

Figure 1. PM emissions rates and cumulative mass emissions for selected PFI, GDI, LDD, and GDI + GPF vehicles for the three-phase FTP.

of all particles 55 nm and larger, and the fit agrees well with experimental data collected up to 350 nm.[45] The density of particles smaller than 55 nm is assumed equivalent to the calculated value at 55 nm, which generally fits measured data[25] and agrees with the empirical approach for calculating coefficients c and D_m based on fractal aggregate theory.[46] The same effective density function was used for all speed-time trace points because the majority of the FTP cycle lay within similar operational windows of power; the application of time-resolved functions based on various steady-state loads had less than a one percent impact on final mass estimates even for LDD vehicles, for which effective density is a stronger function of engine load than gasoline vehicles. Moreover, the selection of an accurate effective density function for a vehicle technology is critical for IPSD to yield accurate mass estimates. This paper uses separate effective density functions for each vehicle technology as recently defined,[30] which are presented in Figure S2 in Supporting Information.

3. RESULTS AND DISCUSSION

3.1. Real-Time PM Mass and Size Distribution. Figure 1 presents real-time and normalized cumulative IPSD mass for the following selected FTP tests of each engine technology: one PFI (2011 Nissan Altima, M_{GRAV} = 0.99 mg/mi), one GDI (2010 Volkswagen Jetta, M_{GRAV} = 1.69 mg/mi), the same GDI retrofit with a prototype gasoline particulate filter (GPF) (M_{GRAV} = 0.22 mg/mi), and one LDD (2013 Volkswagen Jetta TDI, M_{GRAV} = 0.11 mg/mi). The emission of gasoline vehicles was the maximum during the first acceleration of the FTP at a rate of 0.4 mg/sec for the GDI vehicle and between 0.1 and 0.2 mg/sec for the PFI vehicle. The first 45 s of Phase 1 includes three distinct accelerations, during which approximately 25% and 55% of cumulative PM was emitted from the PFI and GDI vehicle, respectively. These two vehicles were each tested multiple times, and a similar trend of emission was observed during Phase 1 of each repeat test (Figure S3, Supporting Information). Elevated cold start emissions for GDI vehicles have been widely reported,[47−50] and this phenomenon is generally attributable to cylinder wall and piston surface wetting before chamber temperatures are sufficient for rapid evaporation. Although PFI systems typically result in lower overall PM emissions than current GDI systems, Figure 1 shows higher real-time PM emission rates were observed later in the test cycle, such as during the successive accelerations between 800 and 1100 s. In contrast to the gasoline vehicles, the LDD emitted at a near constant rate over the FTP; constant emissions over the FTP cycle is also a characteristic of unfiltered diesel emissions,[51] suggesting the DPF efficiency was constant over this specific test. The impact of emissions attributable to the engine cold-start can be assessed by calculating the ratio between phases 1 and 3 because the driving traces are identical. The ratio averages and standard deviations were 5.9 ± 2.0 for GDI, 2.7 ± 0.9 for PFI, and 1.8 ± 1.9 for LDD. Although the LDD vehicles in this study emitted PM at more constant rates over the phases of the FTP than the PFI or GDI vehicles, this may change as emission control strategies and after treatment component designs evolve to meet future emission standards.

A prototype GPF provided by the Dow Chemical Company was temporarily installed underfloor, downstream of the close-coupled catalyst and relying solely on passive regeneration, on the GDI vehicle, and it reduced weighted FTP emissions by 87% relative to without the GPF. Fill state, or soot loading, strongly impacts removal efficiency; Chan et al. (2014) showed a removal efficiency range of 73−88% for BC comparing an empty to filled GPF.[52] The fill state and regeneration status were unknown at the time of testing. Interestingly, the rate of normalized cumulative emissions during the FTP was identical for the GDI vehicle with and without the GPF (Figure 1), even during cold start conditions, indicating the GPF efficiency was constant over the cycle. Moreover, the MMD and geometric standard deviation (GSD) did not change appreciably as a result of the GPF (Figure S4 and Table S3 in the Supporting Information).

3.2. Tunnel Blank Determination. Tunnel blanks conducted at the HSL laboratories through 2012 indicated tunnel blank filter loadings ranged from 1.8 to 2.5 μg per filter (phase), which contributed to around 0.16 mg/mi for the FTP cycle.[18] The origin of this signal could be due adsorption of gaseous artifact, or other uncertainty associated with the gravimetric method during filter handling. Measurements from the EEPS during a selected tunnel blank corresponded to total

DOI: 10.1021/acs.est.5b00666
Environ. Sci. Technol. 2015, 49, 5618−5627

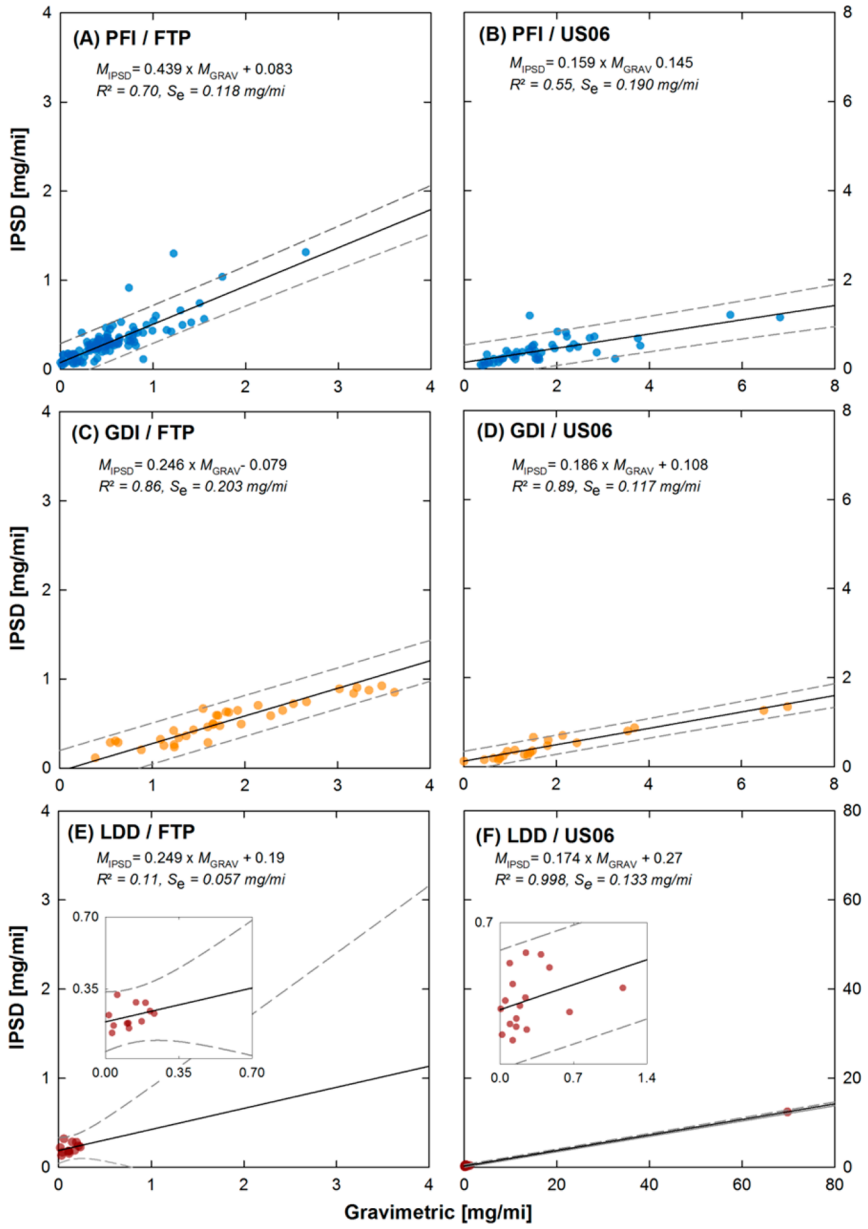

Figure 2. Correlations of M_{IPSD} versus M_{GRAV} for vehicle tests over the FTP (A, C, E), and US06 (B, D, F) test cycles. Dashed lines indicate the 95% prediction intervals, annotations include equations for the best fit lines (least-squares), and fit parameters including R^2 and standard error of the estimate (S_e).

particle number concentrations around 7×10^2 #/cm^3, volume concentrations of 6×10^{-7} cm^3/m^3, and calculated tunnel blank mass (M_{IPSD}) of 0.018 mg/mi (constant ρ_{eff} = 1200 kg/m^3)[30] for standard FTP test conditions (3 phases, 350 CFM). Some test-to-test variation in the number concentration of the EEPS size distribution was observed, but this typically did not span more than a factor of 2. The measured values were all greater than the EEPS detection limit of 170 #/cm^3 calculated using size-resolved RMS noise values provided and derived by TSI from five EEPS units. When accounting for PM larger than the 560 nm EEPS mobility cutoff with a TSI aerodynamic particle sizer (APS, 0.54–2.5 μm) for the same FTP tunnel blank (0.006 mg/mi), the total tunnel background of PM was 0.024 mg/mi, over six times lower than reported by the gravimetric filter-based method. This ratio could change because the availability of EEPS and APS data for the same test was limited, and also the effective density of tunnel background particles could change due to environmental conditions. Nevertheless, the lower tunnel background level for the IPSD method demonstrates the improved sensitivity of the method when measuring near tunnel background levels for the gravimetric method. An evaluation of EEPS and APS size distributions for multiple laboratories over longer periods of time would be needed to define the equivalent tunnel background level for the IPSD method.

3.3. Comparing IPSD and Gravimetric Mass. Figure 2 presents a series of Pearson Least Squares linear regressions for M_{IPSD} versus M_{GRAV} by vehicle technology for FTP and US06 tests. FTP tests with PM emissions exceeding 4 mg/mi were excluded for the linear correlation only, in order to focus on compliant and marginally compliant vehicles to the LEV III standards. A correlation was not reported for the GDI vehicle with a retrofit GPF because only two tests were conducted. Prediction intervals at the 95% confidence level are shown as

DOI: 10.1021/acs.est.5b00666
Environ. Sci. Technol. 2015, 49, 5618–5627

Table 1. Five PFI and Three GDI Vehicles with Eight or More Repeat Tests[a]

ID	vehicle	no. of tests, n	M_{GRAV} (mg/mi)	M_{IPSD} (mg/mi)	correlation, r	S_e (mg/mi)	Pitman-Morgan, t-value	two-sided, p-value
PFI								
A	2013 Dodge Caravan	10	0.13 ± 0.06	0.16 ± 0.01	−0.65	0.011	10.4	<0.01*
B	2011 Nissan Altima	17	0.68 ± 0.24	0.35 ± 0.11	0.84	0.062	1.10	0.210
C	2012 Honda Civic	14	0.61 ± 0.13	0.33 ± 0.05	0.89	0.026	2.20	0.043*
D	2012 GM Malibu	14	0.38 ± 0.09	0.28 ± 0.05	0.54	0.037	1.20	0.187
E	2009 Toyota Camry	14	0.54 ± 0.14	0.35 ± 0.14	0.36	0.143	−2.55	0.024
GDI								
F	2009 μ_BW 335i	9	1.20 ± 0.51	0.40 ± 0.13	0.78	0.087	0.78	0.174
G	2009 μ_BW 750i	8	2.60 ± 0.86	0.70 ± 0.25	0.99	0.046	−1.09	0.204
H	2010 Volkswagen Jetta	17	1.82 ± 0.78	0.51 ± 0.23	0.91	0.104	−0.30	0.374

[a]Standard deviations of the means are indicated following the (±) symbol. Asterisks (*) indicate statistical significance at the 0.05 level.

dashed lines. The standard error of the estimate (S_e) is reported for each panel, which quantifies the average residual error, in units of the dependent variable (M_{IPSD}) in the vertical direction from the best fit line.

3.3.1. Goodness of Fit. PFI and GDI vehicles showed good agreement between IPSD and gravimetric measurements for FTP (R^2 = 0.70 and 0.86, respectively) and US06 (R^2 = 0.55 and 0.89, respectively) tests. Measurements generally lay within the 95% prediction intervals; the average residual error indicated by S_e ranged from 0.12 to 0.19 mg/mi for PFI, and from 0.12 to 0.20 for GDI vehicles. Measurements over the US06 cycle showed better agreement for GDI vehicles compared to PFI vehicles in terms of R^2 and S_e, indicating that measurements were more predictable when characterizing emissions from GDI vehicles. For the FTP cycle, GDI vehicles only showed better fit in terms of R^2 but not S_e, suggesting improved characterization of vehicles with higher emissions, but not necessarily tests with lower emissions because the average of the residuals was greater when weighting all tests equally.

LDD vehicles exhibited weaker correlation between the methods (R^2 = 0.11) compared to gasoline vehicles for FTP tests. One US06 test included an active DPF regeneration (M_{GRAV} = 69.7 mg/mi, ID = 251 in the Supporting Information), resulting in a strong apparent correlation (R^2 = 0.998). This regression analysis violates the assumption that variance is equal across the range of values evaluated; but, it demonstrates how R^2 alone is not always a useful parameter to assess goodness of fit. In this case, the average residual error indicated by S_e was 0.057 and 0.133 mg/mi for the FTP and US06 tests respectively, indicating that the FTP tests exhibited better fit when giving equal weight to each datum. It is important to consider test ID 251 in the analysis because it demonstrates the linearity and application of IPSD to vehicles with PM emissions meeting the LEV III standards and during off-cycle events such as DPF regeneration. When removing the single US06 test including a DPF regeneration, and evaluating the correlation of the clustered data between 0.1 and 0.2 mg/mi, a worse fit (R^2=0.07) was observed. This uncertainty could originate from unpredictable effective density function for LDD, measurement and formation of nonrefractory PM fraction, or measurement uncertainty resulting from measuring vehicle emissions below gravimetric tunnel background levels.

3.3.2. Understanding Methodological Bias. Theoretically, M_{IPSD} and M_{GRAV} should be equivalent, and a one-to-one relationship would result in a slope near unity. However, as shown in Figure 2, M_{IPSD} was virtually always lower than M_{GRAV}. Predictive slopes ranged from 0.25 to 0.44 over the FTP and 0.16−0.19 over the US06. These ranges are lower than our previous evaluation of a smaller data set (slope = 0.63), which included multiple vehicle technologies with PM emissions up to 6 mg/mi.[48] However, the slope of 0.63 was impacted by a single test with $M_{GRAV} \approx 6$ mg/mi; the remaining measurements follow a slope more consistent with the results in this study. In contrast to earlier heavy-duty evaluations of IPSD showing good one-to-one agreement with the gravimetric method,[19,20] this work shows IPSD persistently underestimates filter-collected PM mass when applied to a range of light-duty vehicle technologies. Several possible contributing factors were considered to explain why suspended IPSD mass was lower than filter-collected gravimetric mass.

Strategies used to accelerate catalyst light-off following cold start such as late injection and retarded spark timing,[53,54] could change the relative quantities of soot and hydrocarbon emissions, which influence the effective density of PM emissions, for the brief period responsible for a large fraction of total FTP emissions (Figure 1). The hypothesis that particulate effective density is actually higher during cold start than during warmed-up conditions (and is a contributor to IPSD underestimation) would return a lower slope in the M_{IPSD} vs M_{GRAV} relationship for Phase 1 (Cold Start) compared to the identical Phase 3 (Hot Start). Data show that the slope for Phase 1 was at least 60% higher than Phase 3 for gasoline vehicles (Figure S5, Supporting Information), suggesting that cold-start specific effective density was not a major contributor to the observed IPSD underestimation.

Because tunnel blanks were not subtracted from vehicle tests, the y-intercept of the linear regression can be used to better understand the interaction of volatile constituents on filter media that are not measured by the IPSD method. Using this approach, there was no indication of either gaseous adsorption or evaporation from filter media for gasoline vehicles because all positive and negative intercepts were within the uncertainty of the best-fit line between the two methods. Figure 2 shows the magnitude of the intercepts was within the scatter of the data expressed by S_e. For FTP tests, the intercept ranged from −0.0709 to 0.083 mg/mi, and the S_e ranged between 0.118 and 0.203 mg/mi; and for US06 tests the intercept ranged from 0.108 to 0.145 mg/mi, and S_e ranged 0.117 and 0.190 mg/mi. Although the intercept-based approach indicates gaseous adsorption onto filters was not occurring at very low PM emission levels, gaseous adsorption onto filter media could be proportional to PM emissions. Therefore, at higher emission levels, gaseous adsorption could occur more greatly than at lower emission levels, and be a contributor to the observed discrepancy between the measures of suspended IPSD versus filter-based gravimetric mass.

DOI: 10.1021/acs.est.5b00666
Environ. Sci. Technol. 2015, 49, 5618−5627

We previously used a TSI APS for measuring the contribution of particles above the EEPS cutoff of 560 nm and up to 2.5 μm aerodynamic diameter.[30] By aligning the IPSD and gravimetric measurement ranges to the cyclone cutoff, the slope of M_{IPSD} vs M_{GRAV} increased from 0.50 using only the EEPS to 1.03 using the EEPS and APS. Because Supporting Information Figure S4 suggests FTP mass distributions are bimodal with the larger peak centered above the EEPS measurement range, size range is likely the major contributor to the underestimation by IPSD in the present evaluation. Fast-mobility instrumentation such as the Cambustion DMS 500 (Cambustion, Ltd., Cambridge, UK) could report PM mass up to 1000 nm, but it is still limited because it does not measure size distributions between 1 and 2.5 μm. Combining multiple instruments capable of measuring transient exhaust emissions could be used to further evaluate the relationship between IPSD and gravimetric mass over similar size measurement ranges.

3.4. Repeat FTP Testing and Methodological Variance. Table 1 presents five PFI and three GDI vehicles with at least eight repeat tests over the FTP. Figure 3 presents the average (x) and one standard deviation (s) of repeat tests for each vehicle, and the change in the coefficient of variance (COV = s/x) between methods (ΔCOV = COV_{IPSD} − COV_{GRAV}) calculated from the difference in the average s and x for each vehicle. Generally, reduced COV was observed for measurements of M_{IPSD} compared to M_{GRAV}, and the pooled test-to-test variance indicated ΔCOV was −8%, but a wide range of ΔCOV was observed for individual vehicles (−40% to +25%), indicating variability was higher when using IPSD for some vehicles. The statistical significance of reduced test-to-test variability using IPSD compared to gravimetric measurements was evaluated for each vehicle using the Pitman-Morgan test, which is commonly applied to test the assumption of homogeneity of variance for paired-correlated data.[44] The formula for the t-distribution test statistic is presented in eq 3:

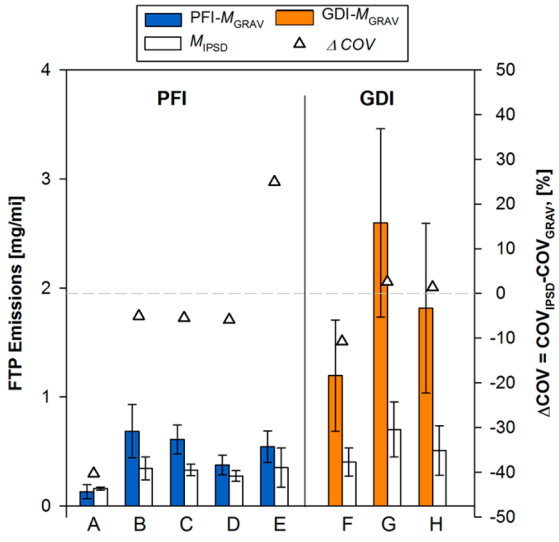

Figure 3. Evaluation of means, standard deviation, and coefficient of variation (COV) between methods for repeat tests of eight or more for five PFI and three GDI vehicles.

$$t = \frac{(F-1)^*\sqrt{(n-2)}}{2\times\sqrt{(F\times(1-r^2))}} \quad (3)$$

where n equals the number of tests, F equals the ratio of the larger versus the smaller variances (e.g., gravimetric to IPSD variance, s^2_{GRAV}/s^2_{IPSD}), and r is the correlation between the methods of the paired data. The Pitman-Morgan Test rejected the null hypothesis of equal variance (H_o: $F = 1$) for all vehicles at the 0.05 alpha level; however, the statistically significant differences in variances were predominately a manifestation of the underestimation of the IPSD method. When accounting for the bias by multiplying the standard deviations of IPSD measurements for each vehicle by the respective ratio of gravimetric to IPSD mass, we were only able to reject the null hypothesis for Vehicle A (p-value <0.001, M_{GRAV} = 0.13 mg/mi) that emitted below the gravimetric tunnel background of 0.16 mg/mi, and Vehicle C (p-value < 0.05, M_{GRAV} = 0.61 mg/mi). For the remaining six vehicles, the IPSD method does not appear to provide a statistically significant reduction in measurement variability. This assumes that measurement variance is proportional to the magnitude of the measurement, and no more or less variance would be observed if a one-to-one agreement were achieved between IPSD and gravimetric methods. Future evaluations of IPSD mass measurement variability should repeat these Pitman-Morgan tests on a data set where a one-to-one relationship is achieved.

Table 1 shows that a strong correlation of M_{IPSD} and M_{GRAV} was observed for all vehicles, ($0.54 < r < 0.99$) except for Vehicle A that had PM emissions below the gravimetric tunnel background. Figure 4 shows a positive correlation between M_{IPSD} and M_{GRAV} for the vehicles above the gravimetric tunnel background (Vehicles C and H). Given these two independent

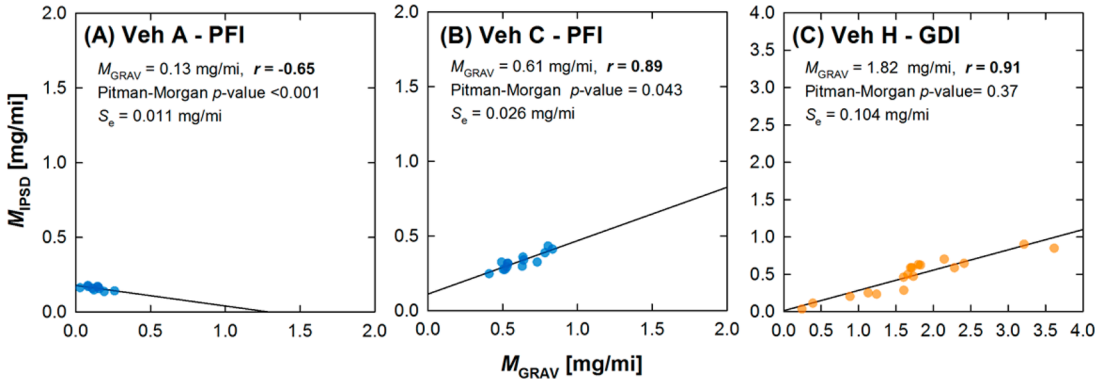

Figure 4. Evaluation of test-to-test variability shown for two PFI vehicles (a,b) and one GDI vehicle (c).

DOI: 10.1021/acs.est.5b00666
Environ. Sci. Technol. 2015, 49, 5618−5627

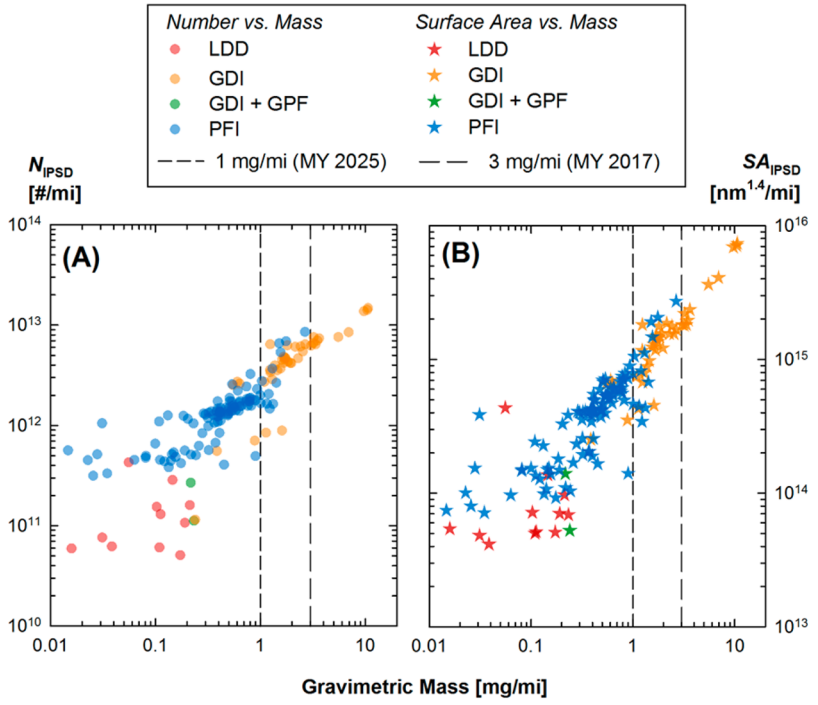

Figure 5. Scatter plots for (a) total particle number, and (b) surface area versus gravimetric PM mass.

measurement approaches show the same trends in test-to-test variability, it suggests the variability does not originate from either measurement method. The correlation parameter r was calculated initially for the Pitman-Morgan tests and, for seven out of eight vehicles, shows how a large fraction of variability originates from actual differences in the vehicle PM emissions rather than the measurement procedure.

The average S_e calculated using repeat tests shown in Table 1 was 0.082 mg/mi including all PFI and GDI vehicles. This average residual for the intravehicle evaluation was smaller than the combined study-pooled PFI (S_e = 0.118 mg/mi) and GDI vehicles (S_e = 0.203 mg/mi). Improved fit when evaluating repeat tests of the same vehicle, as opposed to pooling multiple vehicles using the same engine design technology (e.g., PFI, GDI, or LDD) suggests the accuracy of the mass yielded by IPSD could be influenced by characteristics of emissions from different individual vehicles, at least when referencing gravimetric measurements as the standard. Differences in particulate morphology could result in uncertainty during the conversion of electrometer current into size distribution, and similarly could result in minute differences in effective density functions specific to an individual vehicle make-model, either of which could bias the relationship between gravimetric and IPSD mass.

3.5. Evaluating Alternative Metrics. Figure 5 presents estimates of total particle number (N_{IPSD}) and active surface area (SA_{IPSD}) derived from EEPS measurements versus gravimetric mass (M_{GRAV}) over the FTP cycle. The two dashed vertical lines indicate the 1 mg/mi and 3 mg/mi standards that will be implemented starting with MY 2017 and MY 2025, respectively. Data are clustered by engine technology; most GDI vehicles have PM emissions below 3 mg/mi (average 2.65 mg/mi) and most PFI vehicles have PM emissions below 1 mg/mi (average 0.53 mg/mi). The scatter plot shows a trend between both total number or estimated active surface area, and gravimetric PM mass for the FTP cycle; the slope of the linear regression was used to determine the ratio of N_{IPSD}/M_{GRAV} and SA_{IPSD}/M_{GRAV}.

Per unit mass, PFI vehicles (2.76×10^{12} #/mg) emitted higher total particle number emissions than GDI vehicles (1.63×10^{12} #/mg) and both emitted higher than the LDD vehicle (8.74×10^{11} #/mg). These ratios bound the ratio of 2×10^{12} #/mg for total particle number to gravimetric PM reported previously for GDI vehicles.[18,44] The observed trend between total number and gravimetric PM mass emissions measured above 1 mg/mi over the FTP suggests control of particle number could be achieved through mass-based emissions standards (and conversely, that control of mass emissions could be achieved through particle number standards). In some situations, such as high-temperature events as a result of high-load or DPF regeneration, the ratio may deviate from the trends shown in Figure 5.[55,56] Nevertheless, the data suggest both total number and mass emissions are expected to decline when fully implementing the 1 mg/mi mass standard.

One limitation of using real-time methods estimating mass (e.g., IPSD) and number (e.g., the Euro 5/6 solid particle number >23 nm standard) are their sensitivities to upper and lower size cutoffs, respectively. A measurement parameter that appears less sensitive to lower cutoff size is active surface area,[21] which may be also be a more appropriate dose metric than mass for linking PM exposure to adverse health outcomes.[34] Estimates of active surface area ($d^{1.4}$) using EEPS distributions show the contribution of particles with diameters less than 23 nm (the Euro SPN lower cutoff size) decreased relative to estimates of *total* particle number (d^0) for emissions measuring during FTP tests with PM emissions less than 3 mg/mi; the percent contributions decreased from 13.5% to 4.4% for PFI vehicles, from 28.7% to 4.7% for GDI vehicles, and from 23.1% to 1.5% for LDD vehicles as shown in Figure S6 in the Supporting Information. Based on the trends shown in Figure 5, the estimated active surface area to gravimetric mass ratios were 8.64×10^{14} nm$^{1.4}$/mg, 6.84×10^{14} nm$^{1.4}$/mg, and $5.55 \times$

DOI: 10.1021/acs.est.5b00666
Environ. Sci. Technol. 2015, 49, 5618−5627

10^{14} $nm^{1.4}$/mg for PFI, GDI, and LDD vehicles, respectively. The exponent of particle diameter used to estimate active surface area varies by flow regime (continuum versus free molecular) therefore, a reference method (such as using a diffusion charger) is needed to further verify these calculations. Currently, commercially available instruments can also measure the contribution of particles in size bins between 560 nm and 2.5 μm to evaluate the sensitivity of active surface area to the upper size cutoff.

In summary, this paper evaluates the IPSD method using a comprehensive data set of more than 250 tests representing 34 light-duty vehicles. The application of IPSD as a standalone method for regulatory mass measurement is limited by persistent underestimation of gravimetric filter-collected mass (slope = 0.25−0.44 over the FTP, and slope = 0.16−0.19 over the US06). The underestimation of the IPSD method could originate from the limited size range of the TSI EEPS (5.6−560 nm) and also filter sampling artifact from organics condensing onto filters but not being measured by the IPSD method. Uncertainty in the suspended PM mass measured by IPSD could have resulted from the static performance of the EEPS inversion matrix to convert electrometer current into particle size distribution, and the application of predefined effective density functions. Nevertheless, strong covariance between IPSD and gravimetric methods suggest that observed test-to-test emission variability is largely due to actual differences in vehicle PM emissions, and does not originate from measurement procedures. The IPSD method offered an 8% reduction in test-to-test variability as measured by COV, but the majority of vehicles did not exhibit statistical significant reductions in measurement variability. Future investigations of IPSD need to consider a wider range of particle sizes (and achieve alignment with the gravimetric reference measuring up to 2.5 μm), and additionally need to consider methods to overcome source-specific calibrations of fast-sizing spectroscopy converting charge into number distributions, and effective density functions converting number distributions into mass distributions. Alternative measurement methods adopting new operational definitions, where new paradigms could be used to regulate PM using parameters more broadly than calculating mass, may also be useful to control the adverse health impacts of PM. For example, this work presents estimations of active surface area using size distributions measured by the EEPS and how it is less sensitive to lower cutoff diameter than using a particle number approach. Future work could evaluate these or other alternative metrics, which would not require complex inversion or the postprocessing with effective density functions required to obtain mass using the IPSD method, in order to better understand the trends in PM emissions from light-duty vehicles.

■ ASSOCIATED CONTENT

Supporting Information

Tables S1−S3, Figures S1−S6, and Sections S1−S4. The Supporting Information is available free of charge on the ACS Publications website at DOI: 10.1021/acs.est.5b00666.

■ AUTHOR INFORMATION

Corresponding Author

*Phone: +1-916-445-9370; fax: +1-916-324-1556; e-mail: dquiros@arb.ca.gov.

Notes

The authors declare no competing financial interest.

■ ACKNOWLEDGMENTS

We thank the ARB management and staff who assisted during the project plan development and provided laboratory assistance during testing including Mark Fuentes, Wayne McMahon, Pippin Mader, Bruce Frodin, Henry Toutoundjian, Manuel Cruz, Derrick Lee, Huy Khou, Inna Dzhema, Edward Sun, Shiou-Mei Huang and Carlos Aguirre. We also thank Larry Larsen of the Air Quality Planning and Science Division for his consultation during statistical analysis. Disclaimer: The statements and opinions expressed in this paper are solely the authors' and do not represent the official position of ARB. The mention of trade names, products, and organizations does not constitute endorsement or recommendation for use. ARB is a department of the California Environmental Protection Agency. ARB's mission is to promote and protect public health, welfare, and ecological resources through effective reduction of air pollutants while recognizing and considering effects on the economy. ARB oversees all air pollution control efforts in California to attain and maintain health-based air quality standards.

■ REFERENCES

(1) Pope, C. A.; Dockery, D. W. Health effects of fine particulate air pollution: Lines that connect. *J. Air Waste Manage. Assoc.* **2006**, *56* (6), 709−742.

(2) Brook, R. D.; Rajagopalan, S.; Pope, C. A.; Brook, J. R.; Bhatnagar, A.; Diez-Roux, A. V.; Holguin, F.; Hong, Y.; Luepker, R. V.; Mittleman, M. A. Particulate matter air pollution and cardiovascular disease an update to the scientific statement from the American heart association. *Circulation* **2010**, *121* (21), 2331−2378.

(3) Hu, S.; Paulson, S. E.; Fruin, S.; Kozawa, K.; Mara, S.; Winer, A. M. Observation of elevated air pollutant concentrations in a residential neighborhood of Los Angeles California using a mobile platform. *Atmos. Environ.* **2012**, *51* (0), 311−319.

(4) Zhu, Y. F.; Hinds, W. C.; Kim, S.; Sioutas, C. Concentration and size distribution of ultrafine particles near a major highway. *J. Air Waste Manage. Assoc.* **2002**, *52* (9), 1032−1042.

(5) Westerdahl, D.; Fruin, S.; Sax, T.; Fine, P. M.; Sioutas, C. Mobile platform measurements of ultrafine particles and associated pollutant concentrations on freeways and residential streets in Los Angeles. *Atmos. Environ.* **2005**, *39* (20), 3597−3610.

(6) Fenger, J. Urban air quality. *Atmos. Environ.* **1999**, *33* (29), 4877−4900.

(7) Gauderman, W. J.; Vora, H.; McConnell, R.; Berhane, K.; Gilliland, F.; Thomas, D.; Lurmann, F.; Avol, E.; Kunzli, N.; Jerrett, M. Effect of exposure to traffic on lung development from 10 to 18 years of age: A cohort study. *Lancet* **2007**, *369* (9561), 571−577.

(8) Quiros, D. C.; Lee, E. S.; Wang, R.; Zhu, Y. Ultrafine particle exposures while walking, cycling, and driving along an urban residential roadway. *Atmos. Environ.* **2013**, *73* (0), 185−194.

(9) Choi, W.; Hu, S.; He, M.; Kozawa, K.; Mara, S.; Winer, A. M.; Paulson, S. E. Neighborhood-scale air quality impacts of emissions from motor vehicles and aircraft. *Atmos. Environ.* **2013**, *80* (0), 310−321.

(10) *Health Assessment Document for Diesel Engine Exhaust. In United States Environmental Protection Agency*, EPA/600/8−90/057F; U.S. EPA: Washington, DC, 2002.

(11) Hill, J.; Polasky, S.; Nelson, E.; Tilman, D.; Huo, H.; Ludwig, L.; Neumann, J.; Zheng, H.; Bonta, D. Climate change and health costs of air emissions from biofuels and gasoline. *Proc. Natl. Acad. Sci. U. S. A.* **2009**, *106* (6), 2077−2082.

DOI: 10.1021/acs.est.5b00666
Environ. Sci. Technol. 2015, 49, 5618−5627

(12) Lloyd, A. C.; Cackette, T. A. Diesel engines: Environmental impact and control. *J. Air Waste Manage. Assoc.* **2001**, *51* (6), 809−847.
(13) May, A. A.; Nguyen, N. T.; Presto, A. A.; Gordon, T. D.; Lipsky, E. M.; Karve, M.; Gutierrez, A.; Robertson, W. H.; Zhang, M.; Brandow, C.; Chang, O.; Chen, S.; Cicero-Fernandez, P.; Dinkins, L.; Fuentes, M.; Huang, S.-M.; Ling, R.; Long, J.; Maddox, C.; Massetti, J.; McCauley, E.; Miguel, A.; Na, K.; Ong, R.; Pang, Y.; Rieger, P.; Sax, T.; Truong, T.; Vo, T.; Chattopadhyay, S.; Maldonado, H.; Maricq, M. M.; Robinson, A. L. Gas- and particle-phase primary emissions from in-use, on-road gasoline and diesel vehicles. *Atmos. Environ.* **2014**, *88* (0), 247−260.
(14) *Development of Particulate Matter Mass Standards for Future Light-Duty Vehicles*; CARB: Sacramento, CA, December 7, 2011, 2012; p 165.
(15) Chase, R. E.; Duszkiewicz, G. J.; Jensen, T. E.; Lewis, D.; Schlaps, E. J.; Weibel, A. T.; Cadle, S.; Mulawa, P. Particle Mass Emission Rates from Current-Technology, Light-Duty Gasoline Vehicles. *J. Air Waste Manage. Assoc.* **2000**, *50* (6), 930−935.
(16) CARB. *LEV III PM, Technical Support Document, Development of Particulate Matter Mass Standards for Future Light-Duty Vehicles*; CARB: Sacramento, CA, 2011.
(17) Maricq, M. M.; Szente, J.; Loos, M.; Vogt, R. Motor vehicle PM emissions measurement at LEV III levels. *SAE Int. J. Eng.* **2011**, *4* (1), 597−609.
(18) Hu, S.; Zhang, S.; Sardar, S.; Chen, S.; Dzhema, I.; Huang, S.-M.; Quiros, D.; Sun, H.; Laroo, C.; Sanchez, L. J.; Watson, J.; Chang, O. M.-C.; Huai, T.; Ayala, A. *Evaluation of Gravimetric Method to Measure Light-Duty Vehicle Particulate Matter Emissions at Levels below One Milligram per Mile (1 mg/mile)*, SAE Technical Paper 2014-01-1571, 2014.
(19) Liu, Z.; Swanson, J.; Kittelson, D. B.; Pui, D. Y. H. Comparison of methods for online measurement of diesel particulate matter. *Environ. Sci. Technol.* **2012**, *46* (11), 6127−6133.
(20) Liu, Z. G.; Vasys, V. N.; Dettmann, M. E.; Schauer, J. J.; Kittelson, D. B.; Swanson, J. Comparison of strategies for the measurement of mass emissions from diesel engines emitting ultra-low levels of particulate matter. *Aerosol Sci. Technol.* **2009**, *43* (11), 1142−1152.
(21) Swanson, J.; Kittelson, D.; Pui, D.; Watts, W. Alternatives to the gravimetric method for quantification of diesel particulate matter near the lower level of detection. *J. Air Waste Manage. Assoc.* **2010**, *60* (10), 1177−1191.
(22) Zimmerman, N.; Godri Pollitt, K. J.; Jeong, C.-H.; Wang, J. M.; Jung, T.; Cooper, J. M.; Wallace, J. S.; Evans, G. J. Comparison of three nanoparticle sizing instruments: The influence of particle morphology. *Atmos. Environ.* **2014**, *86* (0), 140−147.
(23) Johnson, T.; Caldow, R.; Pocher, A.; Mirme, A.; Kittelson, D. *A New Electrical Mobility Particle Sizer Spectrometer for Engine Exhaust Particle Measurements*, SAE 2004-01-1341, 2004.
(24) Asbach, C.; Kaminski, H.; Fissan, H.; Monz, C.; Dahmann, D.; Mülhopt, S.; Paur, H.; Kiesling, H.; Herrmann, F.; Voetz, M.; Kuhlbusch, T. J. Comparison of four mobility particle sizers with different time resolution for stationary exposure measurements. *J. Nanopart. Res.* **2009**, *11* (7), 1593−1609.
(25) Maricq, M. M.; Xu, N. The effective density and fractal dimension of soot particles from premixed flames and motor vehicle exhaust. *J. Aerosol Sci.* **2004**, *35* (10), 1251−1274.
(26) Virtanen, A.; Ristimäki, J.; Marjamäki, M.; Vaaraslahti, K.; Keskinen, J.; Lappi, M., Effective density of diesel exhaust particles as a function of size. SAE Technical Paper 2002-01-0056, 2002.
(27) Ristimäki, J.; Virtanen, A.; Marjamäki, M.; Rostedt, A.; Keskinen, J. On-line measurement of size distribution and effective density of submicron aerosol particles. *J. Aerosol Sci.* **2002**, *33* (11), 1541−1557.
(28) Hand, J. L.; Kreidenweis, S. M. A new method for retrieving particle refractive index and effective density from aerosol size distribution data. *Aerosol Sci. Technol.* **2002**, *36* (10), 1012−1026.
(29) Quiros, D. C.; Yoon, S.; Dwyer, H. A.; Collins, J. F.; Zhu, Y.; Huai, T. Measuring particulate matter emissions during parked active diesel particulate filter regeneration of heavy-duty diesel trucks. *J. Aerosol Sci.* **2014**, *73* (0), 48−62.
(30) Quiros, D. C.; Hu, S.; Hu, S.; Lee, E. S.; Sardar, S.; Wang, X.; Olfert, J. S.; Jung, H. S.; Zhu, Y.; Huai, T. Particle effective density and mass during steady-state operation of GDI, PFI, and diesel passenger cars. *J. Aerosol Sci.* **2015**, *83* (0), 39−54.
(31) Donaldson, K.; Stone, V.; Clouter, A.; Renwick, L.; MacNee, W. Ultrafine particles. *Occup. Environ. Med.* **2001**, *58* (3), 211−216.
(32) *Understanding the Health Effects of Ultrafine Particles, Health Effects Institute, HEI Perspectives 3*; HEI, 2013.
(33) Wichmann, H. E.; Spix, C.; Tuch, T.; Wölke, G.; Peters, A.; Heinrich, J.; Kreyling, W.; Heyder, J. *Daily Mortality and Fine and Ultrafine Particles in Erfurt, Germany. Part I: Role of Particle Number and Particle Mass*, Report 98; Health Effects Institute (HEI), 2000.
(34) Sager, T. M.; Castranova, V. Surface area of particle administered versus mass in determining the pulmonary toxicity of ultrafine and fine carbon black: Comparison to ultrafine titanium dioxide. *Part. Fibre Toxicol.* **2009**, *6* (15), 1−11.
(35) Wilson, W. E.; Stanek, J.; Han, H.-S.; Johnson, T.; Sakurai, H.; Pui, D. Y. H.; J, T.; Chen, D.-R.; Duthie, S. Use of the electrical aerosol detector as an indicator of the surface area of fine particles deposited in the lung. *J. Air Waste Manage. Assoc.* **2007**, *57* (2), 211−220.
(36) Jung, H.; Kittelson, D. B. Characterization of aerosol surface instruments in transition regime. *Aerosol Sci. Technol.* **2005**, *39* (9), 902−911.
(37) Kaminski, H.; Kuhlbusch, T. A. J.; Rath, S.; Götz, U.; Sprenger, M.; Wels, D.; Polloczek, J.; Bachmann, V.; Dziurowitz, N.; Kiesling, H.-J.; Schwiegelshohn, A.; Monz, C.; Dahmann, D.; Asbach, C. Comparability of mobility particle sizers and diffusion chargers. *J. Aerosol Sci.* **2013**, *57* (0), 156−178.
(38) Engine testing procedures. In *Code of Federal Regulations*, 40 CFR 1065, 2011.
(39) U.S. EPA. Vehicle-testing procedures. In *Code of Federal Regulations*, 40 CFR 1066, 2012.
(40) Wang, J.; Storey, J.; Domingo, N.; Huff, S.; Thomas, J.; West, B. Studies of diesel engine particle emissions during transient operations using an engine exhaust particle sizer. *Aerosol Sci. Technol.* **2006**, *40* (11), 1002−1015.
(41) Kittelson, D. B.; Watts, W. F.; Johnson, J. P.; Rowntree, C.; Payne, M.; Goodier, S.; Warrens, C.; Preston, H.; Zink, U.; Ortiz, M.; Goersmann, C.; Twigg, M. V.; Walker, A. P.; Caldow, R. On-road evaluation of two diesel exhaust aftertreatment devices. *J. Aerosol Sci.* **2006**, *37* (9), 1140−1151.
(42) Jeong, C.-H.; Evans, G. J. Inter-comparison of a fast mobility particle sizer and a scanning mobility particle sizer incorporating an ultrafine water-based condensation particle counter. *Aerosol Sci. Technol.* **2009**, *43* (4), 364−373.
(43) Wang, X.; Grose, M.; Caldow, R.; Swanson, J.; Watts, W.; Kittelson, D. In *Improvement of Engine Exhaust Particle Sizer Spectrometer for Engine Emissions Measurement*, American Association for Aerosol Research: Minneapolis, MN, 2009.
(44) Keller, A.; Fierz, M.; Siegmann, K.; Siegmann, H. C.; Filippov, A. Surface science with nanosized particles in a carrier gas. *J. Vac. Sci. Technol., A* **2001**, *19* (1), 1−8.
(45) Dwyer, H.; Quiros, D.; Burnitzki, M.; Riemersma, R.; Chernich, D.; Collins, J.; Herner, J. *Ambient Emissions Measurements from Parked Regeneration of 2007 and 2010 Diesel Particulate Filters*, SAE Technical Paper 2014-01-2353, 2014.
(46) Sorensen, C. M. The mobility of fractal aggregates: A review. *Aerosol Sci. Technol.* **2011**, *45* (7), 765−779.
(47) Maricq, M. M.; Szente, J. J.; Adams, J.; Tennison, P.; Rumpsa, T. Influence of mileage accumulation on the particle mass and number emissions of two gasoline direct injection vehicles. *Environ. Sci. Technol.* **2013**, *47* (20), 11890−11896.
(48) Li, Y.; Xue, J.; Johnson, K.; Durbin, T.; Villela, M.; Pham, L.; Hosseini, S.; Zheng, Z.; Short, D.; Karavalakis, G. *Determination of*

DOI: 10.1021/acs.est.5b00666
Environ. Sci. Technol. 2015, 49, 5618−5627

Suspended Exhaust PM Mass for Light-Duty Vehicles, SAE Technical Paper 2014-01-1594, 2014

(49) Samuel, S.; Hassaneen, A.; Morrey, D. *Particulate Matter Emissions and the Role of Catalytic Converter during Cold Start of GDI Engine*, SAE Technical Paper 2010-01-2122, 2010.

(50) Zhang, S.; McMahon, W.; Frodin, B.; Toutoundijan, H.; Cruz, M. Particulate Emissions from California LEV II Certified Gasoline Direct Injection Vehicles. In *20th CRC On-Road Vehicle Emissions Workshop*, San Diego, CA, 2010.

(51) Maricq, M. M.; Podsiadlik, D. H.; Chase, R. E. Examination of the size-resolved and transient nature of motor vehicle particle emissions. *Environ. Sci. Technol.* **1999**, *33* (10), 1618−1626.

(52) Chan, T. W.; Meloche, E.; Kubsh, J.; Brezny, R. Black carbon emissions in gasoline exhaust and a reduction alternative with a gasoline particulate filter. *Environ. Sci. Technol.* **2014**, *48* (10), 6027−6034.

(53) Bielaczyc, P.; Merkisz, J. *Euro III/Euro IV Emissions-A Study of Cold Start and Warm up Phases with a SI (Spark Ignition) Engine*; SAE Technical Paper 1999-01-1073, 1999.

(54) Yi, S.-J.; Kim, H. K.; Quelhas, S.; Giler, C.; Dang, D.; Kim, S. B. *Investigation of a Catalyst and Engine Management Solution to Meet LEV III-SULEV with Reduced PGM*, SAE Technical Paper 2014-01-1506, 2014.

(55) Dwyer, H.; Ayala, A.; Zhang, S.; Collins, J.; Huai, T.; Herner, J.; Chau, W. Emissions from a diesel car during regeneration of an active diesel particulate filter. *J. Aerosol Sci.* **2010**, *41* (6), 541−552.

(56) Herner, J. D.; Hu, S.; Robertson, W. H.; Huai, T.; Collins, J. F.; Dwyer, H.; Ayala, A. Effect of advanced aftertreatment for PM and NOx control on heavy-duty diesel truck emissions. *Environ. Sci. Technol.* **2009**, *43* (15), 5928−5933.

DOI: 10.1021/acs.est.5b00666
Environ. Sci. Technol. 2015, 49, 5618−5627